Lithos 106 (2008) 351–364

Contents lists available at ScienceDirect

Lithos

journal homepage: www.elsevier.com/locate/lithos

$^{40}Ar/^{39}Ar$-ages of phlogopite in mantle xenoliths from South African kimberlites: Evidence for metasomatic mantle impregnation during the Kibaran orogenic cycle

Jens Hopp [a,*], M. Trieloff [a], G.P. Brey [b], A.B. Woodland [b], N.S.C. Simon [c,d], J.R. Wijbrans [d], W. Siebel [e], E. Reitter [e]

[a] Mineralogisches Institut, Universität Heidelberg, Im Neuenheimer Feld 236, D-69120 Heidelberg, Germany
[b] Institut für Mineralogie, Universität Frankfurt, Altenhöferallee 1, D-60438 Frankfurt, Germany
[c] Institute of Physics, University of Oslo, 1048 Blindern 0316 Oslo, Norway
[d] Institute of Earth Sciences, Vrije Universiteit, De Boelelaan 1085, 1081HV Amsterdam, The Netherlands
[e] Institut für Geowissenschaften, Universität Tübingen, Wilhelmstrasse 56, D-72074 Tübingen, Germany

ARTICLE INFO

Article history:
Received 19 May 2008
Accepted 12 September 2008
Available online 20 September 2008

Keywords:
Cratonic lithosphere
Ar–Ar dating
Metasomatism
Southern Africa

ABSTRACT

We applied the $^{40}Ar/^{39}Ar$ dating method to an extensive suite of phlogopites from kimberlite-hosted mantle xenoliths (dominantly garnet bearing) from the mines of Bultfontein (South Africa), Letseng-la-Terae and Liqhobong (Lesotho). Argon extraction was performed by conventional high resolution stepwise heating technique, laser incremental heating technique and laser spot analysis. All age spectra obtained by conventional analysis indicate various degrees of ^{40}Ar loss during kimberlite emplacement, but never resulted in a total reset of the argon system. Most intriguingly, the sample-specific maximum apparent ages cluster between 1.0 and 1.22 Ga for the phlogopites with the least disturbed age spectra. A maximum apparent age of 1.02 Ga was observed during laser heating analysis. Individual grains tend to yield older ages in their cores, with successively younger ages at their rims. The range in age obtained via the laser fusion technique and with conventional stepwise heating technique agrees with each other, as well as with literature data. The often inferred presence of excess ^{40}Ar in those phlogopites cannot explain the coherent age pattern in the large suite of samples. Hence, the age constraint of 1.0–1.25 Ga is regarded as geologically meaningful and assigned to metasomatism of the local cratonic mantle during the advent of Kibaran orogenesis (1.00–1.25 Ga). The major consequences of our findings are: (i) The argon system of phlogopite can remain closed for long time scales, even at ambient temperatures of 800–1200 °C within the mantle, most likely because the solid/solid partitioning behaviour of Ar between phlogopite and other major phases in the mantle strongly favours phlogopite, or because conventionally inferred diffusivity of argon in phlogopite is seriously overestimated. Thus, the $^{40}Ar/^{39}Ar$ phlogopite system appears to be a valuable tool for deciphering ancient metasomatic events affecting the lithospheric mantle. (ii) The cratonic lithospheric mantle below southern Africa may have been frequently influenced by different episodes of fluid or melt migration during subduction of oceanic crust at active continental margins.

1. Introduction

Since Archean times the evolution of the continental lithosphere has been characterized by amalgamation and disintegration of terranes and magmatism during the course of orogenic cycles leading to successive growth of the respective cratonic blocks. This is reflected in the history of the Kaapvaal craton, southern Africa (Fig. 1). Late Archean and Proterozoic-age mobile belts were episodically accreted onto a mid-Archean-aged core, considerably extending the continental lithosphere. Major geotectonic events include the Limpopo orogeny, that led to amalgamation of the Kaapvaal and Zimbabwe cratons (~ 2.7 Ga), and the Eburnian (~ 2.0–1.7 Ga), Kibaran (~ 1.25–1.0 Ga), Pan-African (~ 500 Ma) and Gondwanide (Cape Fold Belt, ~ 280–230 Ma) accretionary events (Thomas et al., 1993). In between these periods of crustal agglomeration continental rifting and rift-related magmatism occurred, particularly during the fragmentation of Gondwana (~ 180–130 Ma). Major magmatic events in southern Africa include the intrusion of the Bushveld Complex (~ 2.0 Ga), the Karroo flood basalts (~ 190 Ma), and several periods with a high rate of kimberlite emplacement (e.g. in the Kimberley and Lesotho areas, ~ 80–90 Ma ago). All these events could have had an impact on the composition and structure of the cratonic lithospheric mantle keel. In particular, observed local refertilization of initially strongly depleted mantle via introduction of melts and fluids enriched in incompatible elements might be explained by metasomatic processes during the Archean or Proterozoic (Pearson et al., 2003). This metasomatism may

* Corresponding author. Tel.: +49 6221 544895; fax: +49 6221 544805.
E-mail address: jhopp@min.uni-heidelberg.de (J. Hopp).

0024-4937/$ – see front matter © 2008 Elsevier B.V. All rights reserved.
doi:10.1016/j.lithos.2008.09.001

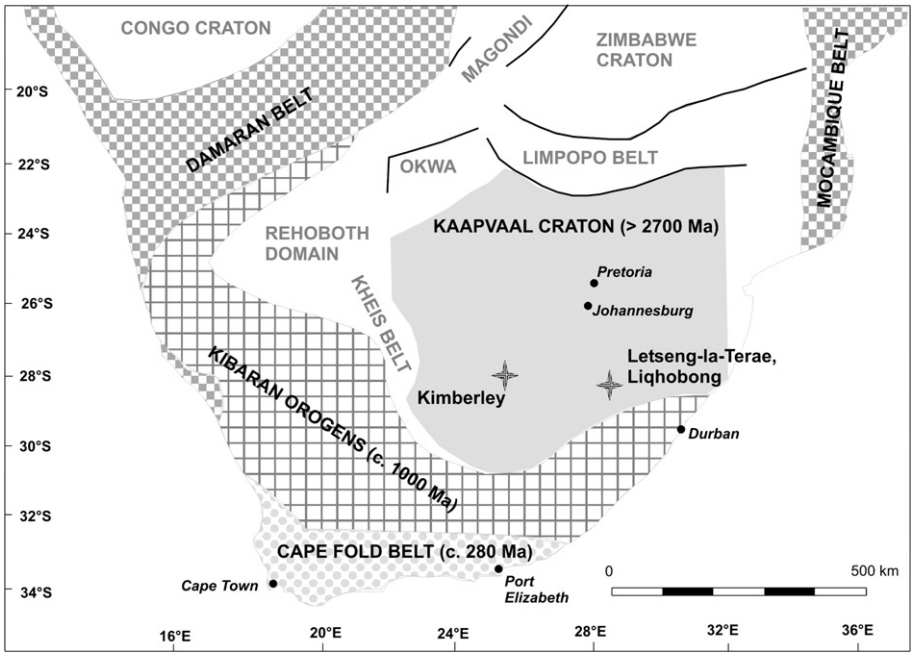

Fig. 1. Geotectonic map of southern Africa with locations of sampled kimberlite pipes of Bultfontein (South Africa), Letseng-la-Terae and Liqhobong (both Lesotho) (modified from Thomas et al., 1993). The latter two are emplaced close to the tectonic border between the Archean Kaapvaal Craton and the Mesoproterozoic Natal Fold Belt.

have been responsible for the formation of diamond and phlogopite within the mantle at different times.

Phlogopite is a possible candidate to determine the time of a metasomatic imprint and its potential association with major geotectonic events. Previous studies showed that $^{40}Ar/^{39}Ar$ ages of phlogopite in mantle xenoliths (garnet peridotites, phlogopite nodules, e.g. Kaneoka and Aoki, 1978; Phillips and Onstott, 1988; Pearson et al., 1997; Johnson and Phillips, 2003) are significantly older than the emplacement age of the kimberlite host. This was often ascribed to the presence of excess (mantle) ^{40}Ar (Kaneoka and Aoki, 1978; Phillips and Onstott, 1986, 1988; Johnson and Phillips, 2003). More recently, $^{40}Ar/^{39}Ar$ ages of phlogopite from Siberian kimberlites were partly interpreted as relict ages (Pearson et al., 1997). A different view is shared by Kelley and Wartho (2000) who demonstrated that the K–Ar-system can be regarded as a closed system even over extended time scales at temperatures far above the commonly accepted closure temperature of phlogopites (~ 450 °C, e.g. Reiners and Brandon, 2006). The authors argue that since K and Ar are highly incompatible in the major mantle minerals, both elements tend to favour the phlogopite lattice. This interpretation is consistent with results from the Baltic shield, that exhibit a consistent chronology with a variety of dating methods (Kempton et al., 2001). However, Johnson and Phillips (2003) have questioned the relevance of this result for phlogopites from xenoliths in kimberlites. In any case, $^{40}Ar/^{39}Ar$ dating of phlogopite in high pressure mantle rocks has only rarely been applied. This is mainly due to difficulties in interpreting of the obtained age spectra related to late-stage disturbance of the K–Ar system during transport in the host kimberlite. In addition, this late interaction might be different at the scale of a single grain, leading to highly variable ages from different individual grains. Hence, the common application of laser-dating might introduce a statistical bias that could be circumvented by $^{40}Ar/^{39}Ar$-dating of a larger subset of phlogopites with the conventional step-heating method.

In this study we applied the $^{40}Ar/^{39}Ar$ dating method for dating phlogopite from both garnet and spinel-bearing peridotite xenoliths from South Africa and Lesotho. We demonstrate that $^{40}Ar/^{39}Ar$ dating can be a useful tool in deciphering the timing of mantle metasomatism in spite of the high mantle *P–T* conditions, which exceed the commonly assumed closure temperature of Ar in phlogopite.

2. Sample locations

The xenoliths studied are from the Cretaceous kimberlite pipes at Kimberley, South Africa, and Letseng-la-Terae and Liqhobong, Lesotho (Fig. 1). The latter two kimberlite pipes intruded into the Tugela

Table 1
P–T conditions of xenolith samples

Sample	Rock type	*P* [GPa]	*T* [°C]
02 Bult 2	Grt-lherzolite	3.20 [BK90]	850 [BK90]
02 Bult 5	Spl-lherzolite	–	–
02 Bult 6	Grt-lherzolite	3.25 [BK90]	845 [BK90]
02 Bult 7	Grt-lherzolite	2.93 [BK90]	815 [BK90]
02 Bult 9	Cpx-Megacryst	–	–
Kim 1[a]	Grt-lherzolite	4.37 [BK90]	1112 [BK90]
Kim 3	Spl-lherzolite	–	–
Kim 5[a]	Grt-harzburgite	4.26 [BK90]	1082 [L95]
Kim 8[a]	Spl-harzburgite	<4.60[b]	997 [BK90]
Kim 9	Spl-amphibole lherzolite	–	–
Kim 17[a]	Grt-harzburgite	4.64 [BK90]	1196 [BK90]
Kim 25[a]	Grt-lherzolite	4.30 [BK90]	1048 [BK90]
Kim 31	Grt-harzburgite	–	–
Let 14[a]	Grt-lherzolite	4.45 [BK90]	1108 [BK90]
Let 39[a]	Grt-lherzolite	4.64 [BK90]	1083 [BK90]
Liq 1[a]	Grt-lherzolite	4.63 [BK90]	1157 [BK90]
Liq 9[a]	Spl-harzburgite	<3.00[b]	920 [BK90]
Liq 11[a]	Grt-lherzolite	4.47 [BK90]	1083 [BK90]
K 3[c]	Grt-lherzolite	4.56 [BK90]	1075 [BK90]
K 5[c]	Phl-peridotite	–	–
K 19[c]	Grt-lherzolite	3.75 [BK90]	925 [BK90]
K 22[c]	Phl-K-richterite peridotite	–	–
Let 2[d]	Grt-harzburgite	3.0 [BK90]	930 [H84]
Let 64[d]	Grt-lherzolite	3.8 [BK90]	990 [H84]

[BK90]: Al-in-opx barometer / 2-px-thermometer, Brey and Köhler (1990); [H84]: grt-opx-thermometer, Harley (1984); [L95]: ol-spl-thermometer, Li et al. (1995).
[a] Woodland and Koch (2003).
[b] Maximum pressure after Carroll Webb and Wood (1986).
[c] Simon et al. (2007).
[d] Simon (2004).

Terrane, a Kibaran-aged allochthon lying between older stratigraphic units close to the southern border of the Kaapvaal craton. The kimberlites penetrated a kilometer-thick pile of Karroo flood basalts that erupted ca. 180 Ma ago (Marsh et al., 1997). The Karroo flood basalts probably extended to the area around Kimberley, but are now absent due to erosion. The Kimberley group pipes were emplaced in late Archean crustal rocks and lie ~ 250 km from the southern and western edge of the Kaapvaal craton (Fig. 1).

3. Samples and analytical details

3.1. Conventional $^{40}Ar/^{39}Ar$-dating

All xenolith samples from the Kimberley Mine group were collected from Boshoff road dump and the megacryst sample, 02 BULT 9, from Pulsator road dump. The majority of these dumps were excavated from the Bultfontein Mine, but some material originated from the other mines of the Kimberley group. Thus, it is impossible to exactly locate the provenance of each rock. The Lesotho xenoliths came from Letseng-la-Terae and Liqhobong. The host kimberlites are of similar age (~ 80–90 Ma, Allsopp and Barrett, 1975; Kramers et al., 1983; Richardson et al., 1985; Smith et al., 1989; Konzett et al., 1998). All kimberlites are group I kimberlites (e.g. Smith, 1983). Most xenolith samples are garnet lherzolites or garnet harzburgites, except Kim 3, Kim 8, Liq 9 and 02 BULT 5, which are spinel peridotites (Table 1). However, Kim 8 shows evidence for metasomatic formation of secondary clinopyroxene and associated spinel. Hence, both phases are considered as breakdown products of garnet (Woodland and Koch, 2003). Equilibrium temperatures and pressures for several xenoliths studied are reported by Woodland and Koch (2003), Simon et al. (2003, 2007) and Simon (2004), and encompass a range of 800–1200 °C and 2.9–4.6 GPa, respectively (Table 1). In addition, we included in our study one diopside megacryst (02 BULT 9) that contains abundant interlayer phlogopites suited for $^{40}Ar/^{39}Ar$-dating.

Phlogopites selected for analyses were generally coarse grained (>300 μm). The modal abundances of phlogopite within its peridotic host was not determined, but judging from mere visual inspection there is a large variation between relatively abundant (e.g. 02 BULT 2) and extremely rare (Liq 11: 6 grains used for analysis; Kim 5: 3 grains used for analysis). We determined the major composition of phlogopites from several xenoliths with electron microprobe analyses. These data are available in supplementary material "compositions of phlogopites". For dating all phlogopites were handpicked under a microscope and subsequently washed ultrasonically with ethanol and dried at 50 °C before wrapping in aluminium foil.

All samples for conventional dating were neutron-irradiated with Cd-shielding for 10days in three separate irradiations at the GKSS reactor in Geesthacht, Germany. Each phlogopite was bracketed by two BMus2 age monitors with an age of 328.5 ± 1.1 Ma (Schwarz and Trieloff, 2007). All conventional argon analyses were performed at the Mineralogical Institute, University of Heidelberg. Before the measurements, the samples were pre-baked at ~ 100 °C for 5days. Gas release was achieved via a cyclic stepwise heating procedure in a resistance heated tantalum crucible (Staudacher et al., 1978). The heating time varied from sample to sample (10 to 20min), but always was kept constant during one individual sample analysis. Hot and cold Ti-sponge and Zr–Al-getters, respectively, were used for cleaning the sample gas. Argon composition was subsequently analysed in a Varian MAT CH5 noble gas mass spectrometer. For correction of analytical mass fractionation we frequently measured a standard gas with isotopic composition of air. Furthermore, we always applied a correction for signal intensity dependent variations of analytical mass fractionation and sensitivity factors (Trieloff et al., 2003). The order of magnitude of this correction is in the range of −0.1 to +0.25% ($^{40}Ar/^{39}Ar$-ratio) and down to − 2.0% (^{40}Ar-concentrations). The blank composition was atmospheric within uncertainties. Blanks of ^{40}Ar reached up to 10^{-8}ccm STP/g at 1500 °C, but were generally below 10^{-9}ccm STP/g at main argon release temperatures <1100 °C. All data can be found in supplementary material "Tables".

Table 2
Sm–Nd data of clinopyroxene–garnet pairs

Sample	Weight (mg)	$^{147}Sm/^{144}Nd$	$^{143}Nd/^{144}Nd$	Nd (ppm)	Sm (ppm)
02 Bult 2 cpx	43.30	0.0937 (5)	0.512048 (10)	50.35	7.803
02 Bult 2 grt	61.12	0.2659 (13)	0.512350 (10)	1.267	0.557
02 Bult 6 cpx	42.36	0.0740 (4)	0.511936 (10)	54.72	6.702
02 Bult 6 grt	60.34	0.2735 (14)	0.512086 (10)	0.894	0.405
02 Bult 7 cpx	47.68	0.0769 (4)	0.511898 (10)	37.94	4.828
02 Bult 7 grt	68.32	0.3877 (19)	0.512621 (10)	0.861	0.552
Garnet–clinopyroxene two-mineral age (Ma)					
02 Bult 2	268 ± 9				
02 Bult 6	115 ± 8				
02 Bult 7	355 ± 6				

3.2. $^{40}Ar/^{39}Ar$-dating with laser techniques

Four garnet peridotites from the Kimberley group mines (Boshoff road dump) and two garnet peridotites from Letseng-la-Terae, were the subject of a laser $^{40}Ar/^{39}Ar$-dating study of phlogopite at Vrije Universiteit, Amsterdam (supplementary material "Tables"). All xenoliths were part of a more extended sample suite. For most xenoliths of this suite petrographic, petrologic and geothermobarometric data, trace element patterns and isotope compositions are available (Irvine et al., 2001; Simon et al., 2003; Simon, 2004; Simon et al., 2007). The age monitor used in $^{40}Ar/^{39}Ar$-dating was Drachenfels sanidine Dra-2 with a standard age of 25.26 ± 0.05 Ma. All data were corrected for blank contributions. Procedure blanks were in the range $(1–2.5)\cdot10^{-18}$ moles ^{40}Ar.

3.3. $^{147}Sm/^{143}Nd$-dating

Three garnet–clinopyroxene pairs were investigated for their Sm–Nd isotopic composition at the University of Tübingen, Germany (Table 2), uncertainties are 1σ-errors. All mineral separates were washed ultrasonically for 10min with diluted nitric acid, deionized water and ethanol. Column separation after spike addition of Sm and Nd followed standard laboratory separation schedules and included a spiked blank sample. Correction for analytical mass fractionation is accounted for by measurement of the La Jolla standard ($^{143}Nd/^{144}Nd_{La\ Jolla}$ = 0.51185). We obtained a $^{143}Nd/^{144}Nd$ = 0.511828. All samples were analysed with a Finnegan MAT 262 mass spectrometer (at Institut für Geowissenschaften, Universität Tübingen).

4. Results

4.1. $^{40}Ar/^{39}Ar$-age spectra (conventional heating technique)

The age spectra (supplementary material "Tables"; Fig. 2A–T) of all phlogopites show a similar form. At the lowest extraction temperatures (i.e. at low percentage of ^{39}Ar release) apparent ages are very old. This is likely a consequence of neutron-induced recoil loss of ^{39}Ar from grain surfaces (Foland and Xu, 1990; Trieloff et al., 1994, 1998). Because grain surfaces are the least retentive sites during heating, these are represented in the first temperature steps and accordingly show drastically elevated $^{40}Ar/^{39}Ar$ ratios. With increasing temperature, apparent ages first decrease (typically during release of first 5% of ^{39}Ar) to a minimum. Evidently, phlogopites with young minimum apparent ages also have younger maximum ages. This results from partial loss of radiogenic $^{40}Ar^*$ during a late thermal event most likely related to kimberlite emplacement. The youngest apparent

ages, 77 ± 1 Ma for Liq 11 and 95 ± 4 Ma yielded by megacryst 02 BULT 9 (without standard error), accordingly define an upper limit of the kimberlite age, in broad agreement with previous age determinations of about 85 ± 5 Ma (Pb–Pb and Rb–Sr ages, Allsopp and Barrett, 1975; Kramers et al., 1983; Richardson et al., 1985; Konzett et al., 1998). The rather young age for the Lesotho sample Liq 11 might reflect a real age difference between both kimberlite pipes. Alternatively, post-emplacement loss of $^{40}Ar^*$ might also apply.

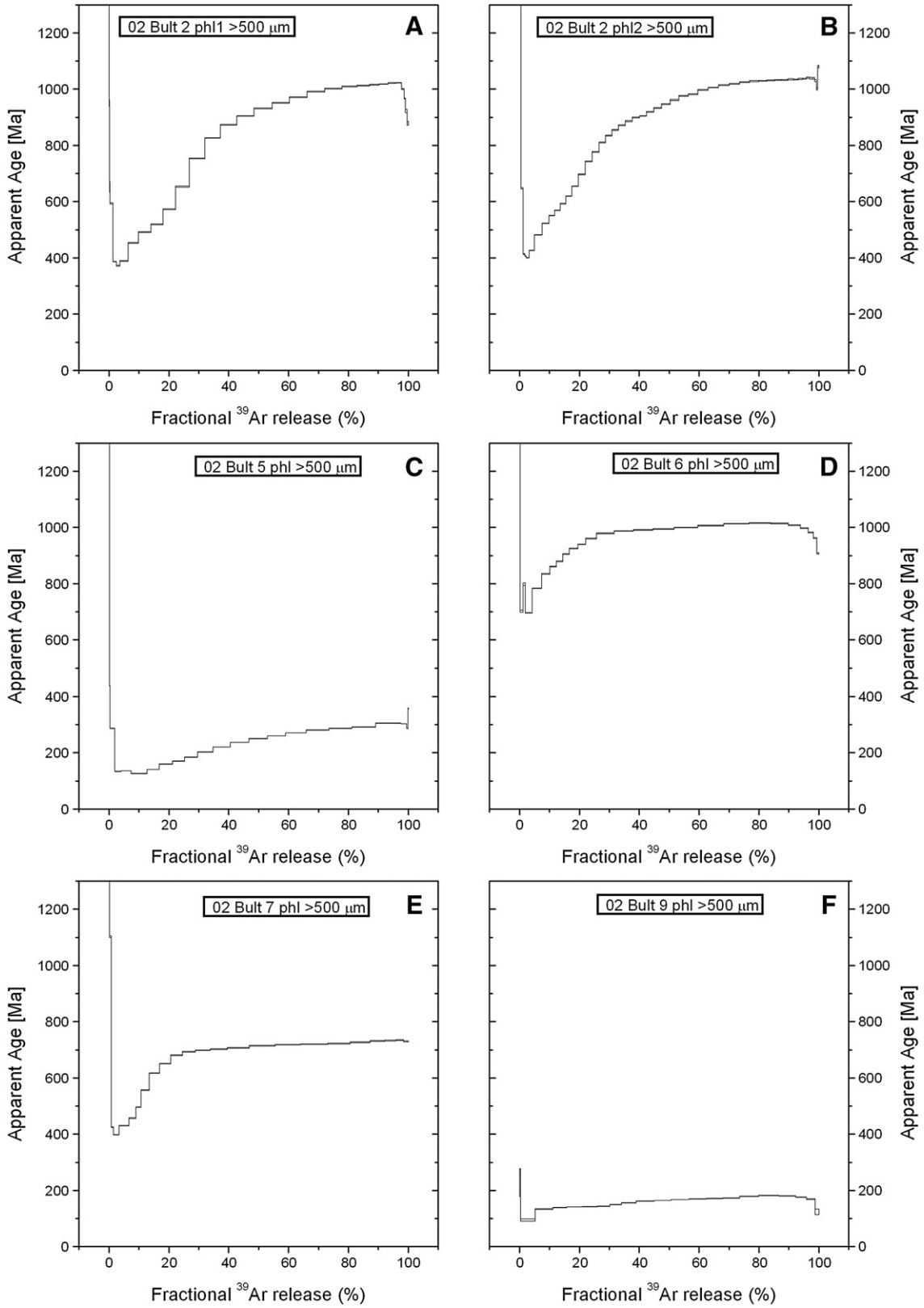

Fig. 2. A–T: Age spectra of phlogopites investigated with conventional $^{40}Ar/^{39}Ar$ dating method. The gap in age spectrum of Kim 1 (G) is due to a system malfunction and respective ^{39}Ar release is estimated from the argon release pattern.

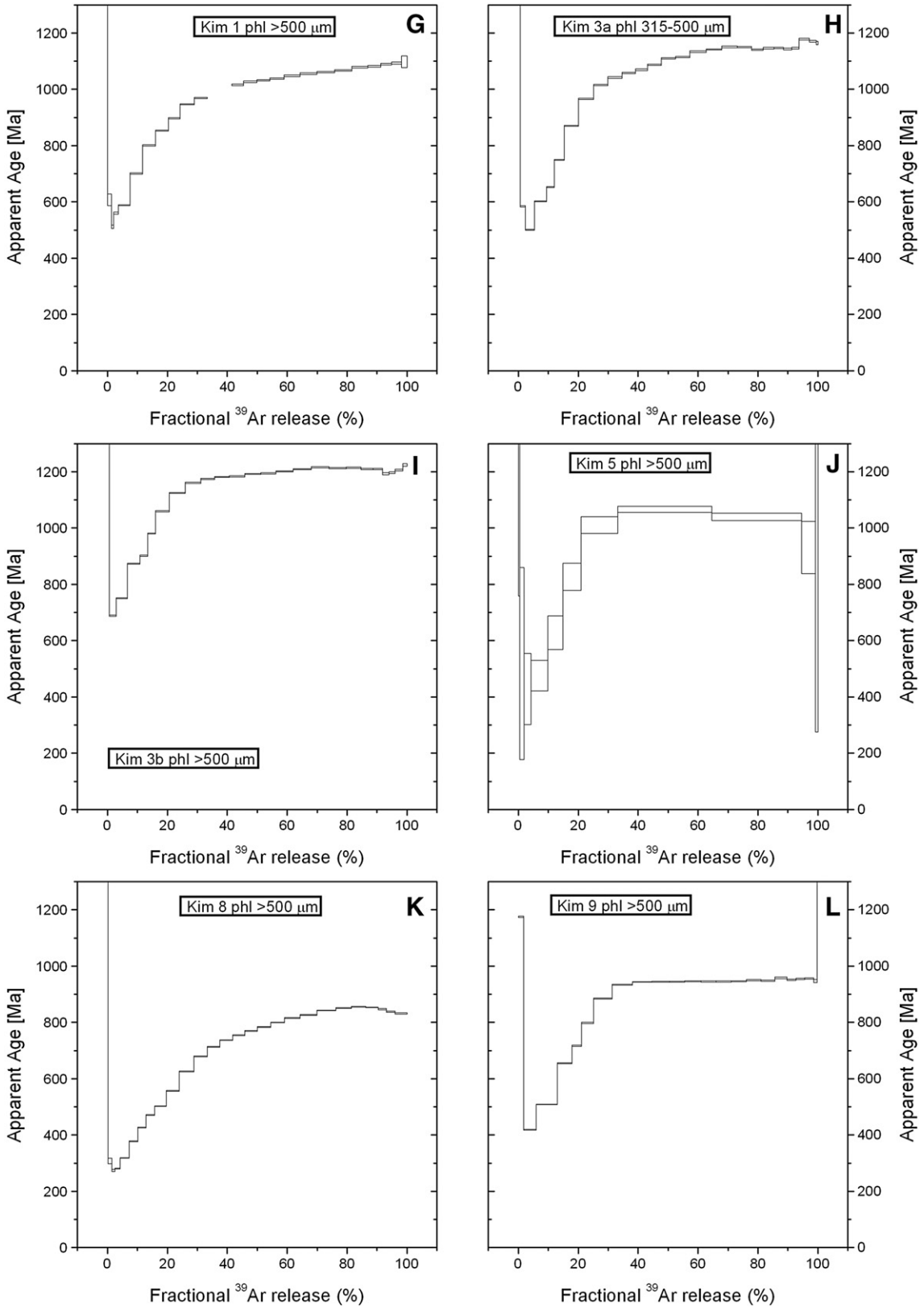

Fig. 2 (*continued*).

The continuous rise of apparent ages rise to more constant values at a higher amount of fractional release in ^{39}Ar is characteristic of age spectra displaying diffusional ^{40}Ar loss, with a steeper trend at lower temperatures and shallower slopes at higher temperatures. If secondary ^{40}Ar* loss is not too severe a flat 'plateau'-like age pattern with several extractions of indistinguishable age can be obtained, dating a geologically meaningful event. This is the case for phlogopite Kim 9 (948±2 Ma, 13 extractions between 910° and 1080 °C). The

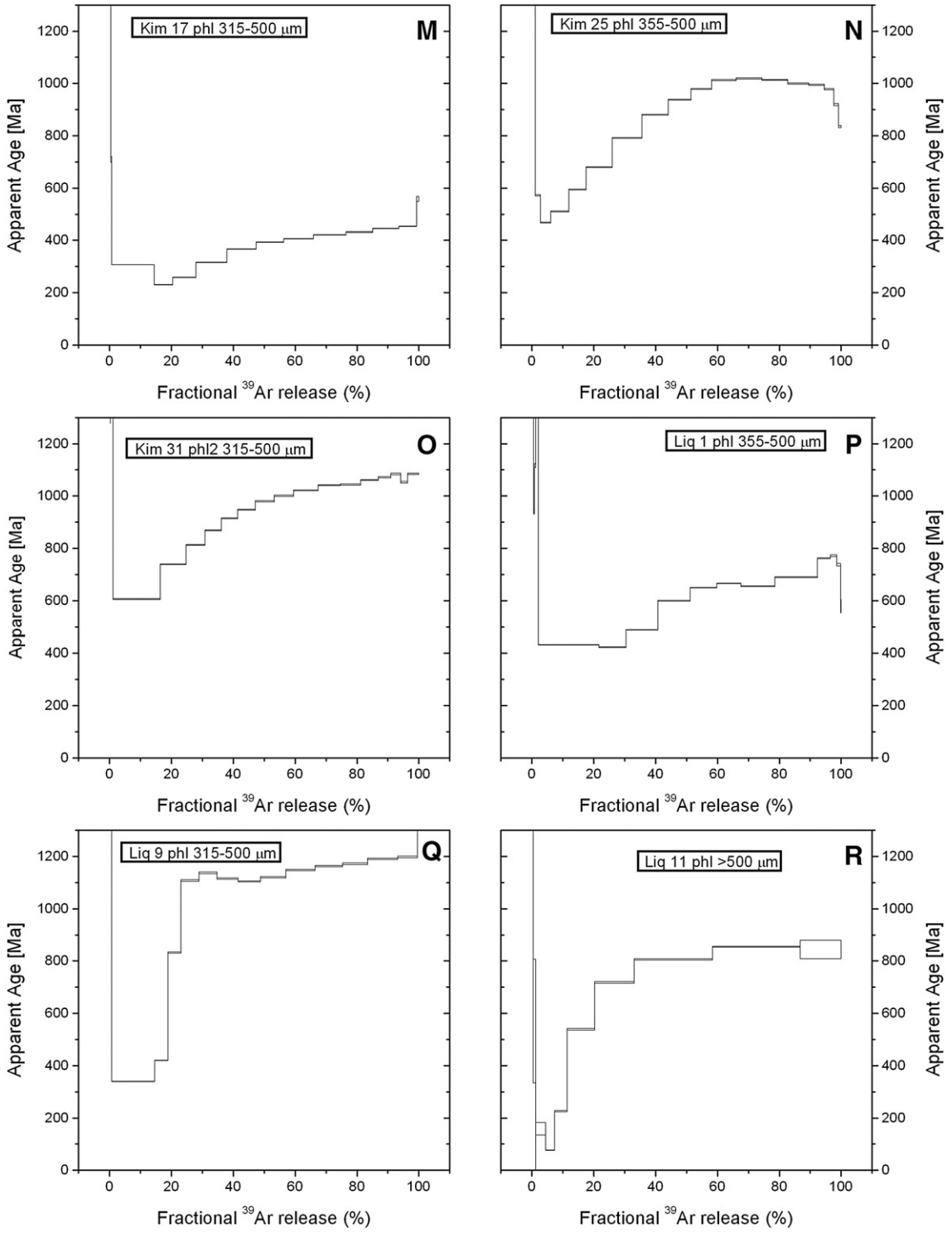

Fig. 2 (*continued*).

spectrum of phlogopite Liq 9 shows a more disturbed age 'plateau' but without sign of significant ^{40}Ar-loss. In this case we consider an integrated age of 1152±52 Ma from respective extractions (930–1300 °C) as more reliable.

Several samples show a disturbance in apparent ages at highest temperatures. The drop is most likely caused by a recoil-induced redistribution of ^{39}Ar into more retentive mineral phases that start to degas at higher temperatures and thus, lead to lower ^{40}Ar/^{39}Ar ratios (=younger apparent ages) at higher temperatures. Major candidates of more retentive minerals that start degassing above 1000 °C are orthopyroxene, garnet, olivine and clinopyroxene (e.g. Trieloff et al., 1997; Hopp and Trieloff, 2005; Hopp et al., 2007). It is indeed observed that some phlogopites are intimately intergrown with other phases that were difficult to recognize under the microscope. At highest temperature (1360–1400 °C) corresponding to the last extraction of a sample, when phlogopite is expected to be thoroughly degassed, several samples show a significantly elevated apparent age. We interpret this as contributions from the more retentive mineral phases that contain mantle or crustal (=excess) ^{40}Ar. Presence of such an excess argon component is corroborated by results of noble gas

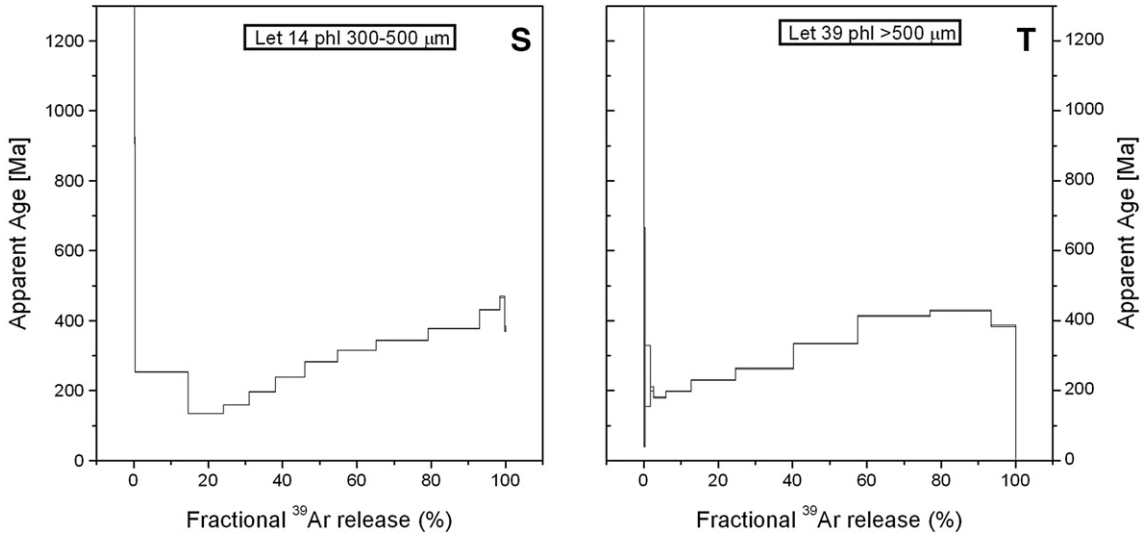

Fig. 2 (*continued*).

measurements for orthopyroxenes contained in some of the dated xenoliths (Hopp and Trieloff, 2008) and by the results of the laser method discussed below. However, note that the total contribution of excess ^{40}Ar in respective phlogopite extractions (Fig. 2B: 02 BULT 2 #2; c: 02 BULT 5; l: Kim 9; m: Kim 17; q: Liq 9) is negligible compared to the total ^{40}Ar concentration. Alternatively, the high apparent ages – observed at highest extraction temperature with small amounts of ^{39}Ar released – could be an artifact resulting from different diffusion coefficients of ^{39}Ar and ^{40}Ar, induced by their different atomic masses and the implicit difference in frequency (preexponential) factors (Trieloff et al., 2005).

For the majority of phlogopites the oldest sample-specific ages (excluding the before-mentioned last extraction of a sample with excess ^{40}Ar and the first extractions affected by recoil-induced ^{39}Ar-loss or redistribution) represent a lower limit for their respective original ^{40}Ar*-loss corrected apparent age. The age distribution of maximum ages within the sample suite, including the 'plateau' ages of Liq 9 and Kim 9, is shown in Fig. 3 (conventional Ar–Ar data). A major age peak at 1.0–1.2 Ga is apparent. This peak is dominated by samples from the Kimberley region but there is no general age difference

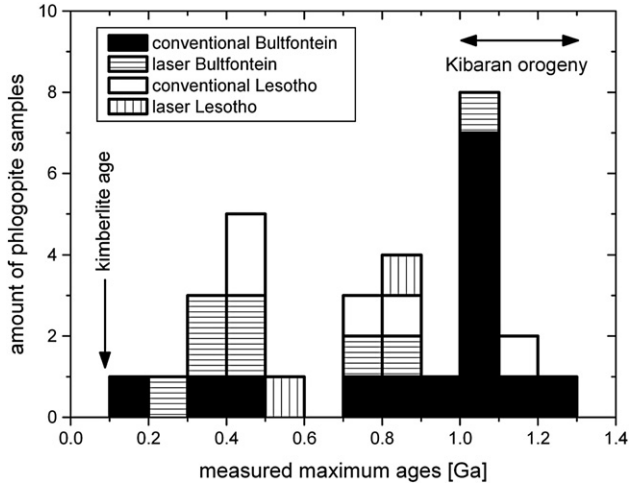

Fig. 3. Histogram showing the relation of maximum ages of phlogopites and their abundance within this sample suite (100 Ma resolution, conventional: 20 phlogopites / 2 duplicates; laser: 10 phlogopites / 4 duplicates). Excluded are data from recoil dominated low-temperature extractions and, for five samples, high-temperature extractions with excess ^{40}Ar hosted in minor impurities (e.g. olivine, pyroxenes). The histogram points to an age clustering around 1.0–1.3 Ga contemporaneous to the Kibaran orogenic cycle (age range indicated by arrow) and far above the age of kimberlite emplacement (ca. 90 Ma).

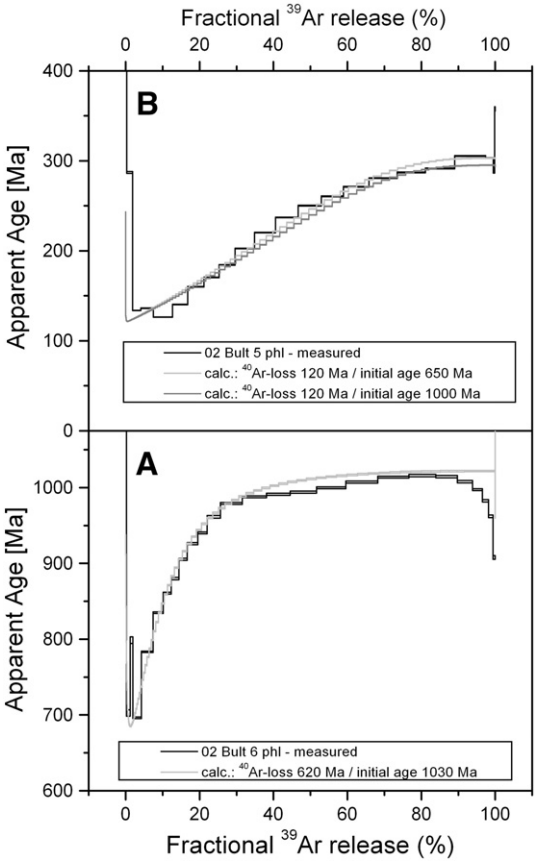

Fig. 4. Comparison of measured (black lines) and simulated (grey lines) age spectra for (A) sample 02 Bult 6 and (B) 02 Bult 5. Ages in legend refer to applied loss age and original age. In case of 02 Bult 6 best fit-loss age is significantly above kimberlite age, and might be an artefact of the simplified model calculation. Both examples of calculated age spectra for 02 Bult 5 are similar in shape, though applied original age is very different.

between phlogopites from Lesotho and Kimberley. In particular, maximum ages of phlogopites from Liqhobong are between 800 and 1150 Ma. Phlogopites with maximum ages coincident with the kimberlite emplacement age of 90 Ma are not present and hence, no sample had been completely reset by the emplacement event.

On the other hand, diffusional ^{40}Ar* loss can significantly decrease the observed maximum ages within an age spectrum, possibly inducing a bias towards low geologically meaningless ages. In order to quantify this bias, we performed a diffusional modelling of age spectra (simple spherical geometry, one K-bearing phase) including recoil-loss of ^{39}Ar (for model details see Trieloff et al., 1994, 1998). Diffusion parameters (activation energy, D_0/a^2 with D_0=frequency factor, a=grain size) are derived from the Ar release patterns and respective Arrhenius plots of individual samples. We used discrete grain sizes for calculations that are derived from modelled recoil-loss of ^{39}Ar (Trieloff et al., 1994, 1998). The overall shape of the calculated age spectra (except the first ca. 5% of ^{39}Ar release) do not depend on this preposition because the essential parameter determined via Arrhenius plots for diffusion modeling is D_0/a^2, i.e. not independent values of grain size and frequency factor. Of course, our calculations imply several approximations and assumptions: For example, they assume spherical grain geometry instead of cylindrical geometry that may more adequately fit the diffusion behaviour of mica (Giletti, 1974), although the difference in modeled age spectra are probably minor. Furthermore, the calculation bases on the assumption that volume diffusion occurs. Since a change in physical and chemical properties of micas (biotites and muscovites, but no phlogopites) during in vacuo step-heating is well documented (e.g. Gaber et al., 1988; Sletten and Onstott, 1998; Lo et al., 2000), in particular delamination and dehydration processes, volume diffusion likely describes only parts of the gas release. Nevertheless, a number of our phlogopite samples – particular the ones we used fore age spectra simulations – display single argon release peaks with shapes expected for a volume diffusion mechanism. In summary, we consider our calculations will only approximate the shift between the original age (before ^{40}Ar*-loss) and the maximum ages of a specific age spectrum. Nevertheless, our general approach appears justified because calculated and measured age spectra agree reasonably well with a volume diffusion model (examples in Fig. 4). The primary original age and the time of secondary disturbance are free fit parameters, the best values are obtained by χ^2 fit routines. It turns out that the phlogopites with the oldest apparent ages (e.g. 02 Bult 2; 02 Bult 6; Kim 3a+b) represent samples suffering a rather low degree of ^{40}Ar* loss. In these cases, the best fit value of the original age hardly deviates from the maximum ages measured in individual extractions, and thus only a small age correction applies. For example, sample 02 Bult 6 yielded a maximum age of 1024±1 Ma and a calculated original age of about 1030 Ma (Fig. 4A). In general, best fit values of original ages never exceeded 1250 Ma. On the other hand, regression analysis for samples with maximum ages significantly younger than 1 Ga were consistent with a larger secondary loss of ^{40}Ar* and resulted in less well constrained original age values. For example, two model spectra for 02 Bult 5 phlogopite shown in Fig. 4B both well fit the measured spectrum, though they assume quite different original ages of 650 and 1000 Ma. These difficulties preclude a graphical visualization in a histogram like Fig. 3 with calculated original ages plotted instead of measured maximum ages.

Only the age calculation for sample 02 Bult 7 yielded a significant best fit original age of 750 Ma. This age differs markedly from the majority of our phlogopites that indicates original ages between 1.0 and 1.25 Ga.

4.2. Ar–Ar spectra (laser technique)

Age spectra obtained by successively increasing laser power (samples K3, K19, Let 2) are shown in Fig. 5A–E. All samples experienced some degree of ^{40}Ar*-loss as indicated by the younger ages obtained in first extraction steps that represent the outer parts of the phlogopite grain. The central region of the phlogopite is degassed at the progressive stages of the experiment and accordingly yields the oldest apparent ages. The individual maximum apparent ages cover a similar range as obtained with conventional stepwise heating, yielding a total maximum of 1019±3 Ma (K 19a; Fig. 5C; supplementary material "Tables"). The youngest age measured with incremental heating technique is 155±2 Ma.

Five phlogopites (Let 64a, K 5a,b; K 22a,b) and one glass phase (Let 64b) were mapped with single spot analysis (supplementary material "Tables" and Supplementary Lasermaps). For each sample, cumulative age spectra ordered in sequence of increasing ages are shown in Fig. 5F–H. The glass and some mineral grains adjacent to it (no phlogopites) gave old apparent ages ranging from 1920±411 Ma to 3094±1213 Ma. Mapping of the phlogopite grains yields results consistent with both the incremental and conventional heating techniques. The core regions tend to give older apparent ages compared to the rims, although in detail this also depends on the distribution of internal cracks. However, the youngest ages are always observed at the grain rims. The ages range from 140±3 Ma to 892±6 Ma and 988±89 Ma and are similar to apparent ages reported above. Two phlogopite grains from the same xenolith sample (K19 a,b, Fig. 5C and D; K5 a,b, h; K22 a,b, g) show distinct minimum and maximum ages; a result that holds for both the incremental heating and the single spot mapping techniques. This requires that individual grains in a xenolith were variably susceptible to thermal and mechanical stress during kimberlite ascent and hence, suffered various degrees of ^{40}Ar* loss.

In summary, the laser heating data also yielded maximum ages up to 1.02 Ga and span the same range found for the phlogopites analysed with the conventional step-heating method (Fig. 3).

4.3. ^{147}Sm/^{143}Nd-ages

For three samples Sm–Nd dating was performed on garnet-clinopyroxene pairs (Table 2). The ages obtained are 268±9 Ma (02 BULT 2), 115±8 Ma (02 BULT 6) and 355±6 Ma (02 BULT 7), which are all younger than the corresponding Ar–Ar ages. These ages are slightly older (02 BULT 2, 02 BULT 7) or similar (02 BULT 6) to the kimberlite emplacement age (80–90 Ma). Evidently, Sm–Nd ages appear to mirror an ancient metasomatic event that led either to formation or modification of the garnet–clinopyroxene pair. The Sm–Nd system was likely disturbed during the kimberlite event, probably by infiltration of melt. This effect was also observed for several other isotope systems (Rb–Sr, Sm–Nd, Lu–Hf, Re–Os) and trace element patterns in xenoliths from Kimberley and Lesotho (Simon et al., 2003; Simon, 2004; Simon et al., 2007).

5. Discussion

As demonstrated above original ages of most analysed phlogopites range between 1.0 and 1.25 Ga, with few exceptions displaying younger original ages. Implicitly we assumed that diffusional ^{40}Ar* loss was related to kimberlite emplacement 90 Ma ago, in broad agreement with observed minimum ages in low-temperature extraction steps. No ages corresponding to the overlying Palaeoproterozoic / Neoarchean crust (at Kimberley) were observed. In the following, we summarize previously reported Ar–Ar ages of phlogopites hosted in kimberlites and their xenoliths from the Kimberley group and Lesotho. These results are in agreement with our findings. We then go on to discuss the following possible age interpretations:

(i) Contributions of an excess ^{40}Ar component in the phlogopites unrelated to ^{40}K-decay, implying that measured ages are without any geochronologic meaning, (ii) Existence of several generations of phlogopite with differing ages, creating mixed ages with a complex geochronologic meaning, (iii) A thermochronologic approach that relates the observed ages to a progressively cooling lithospheric mantle section until closed system conditions for Ar in phlogopite are

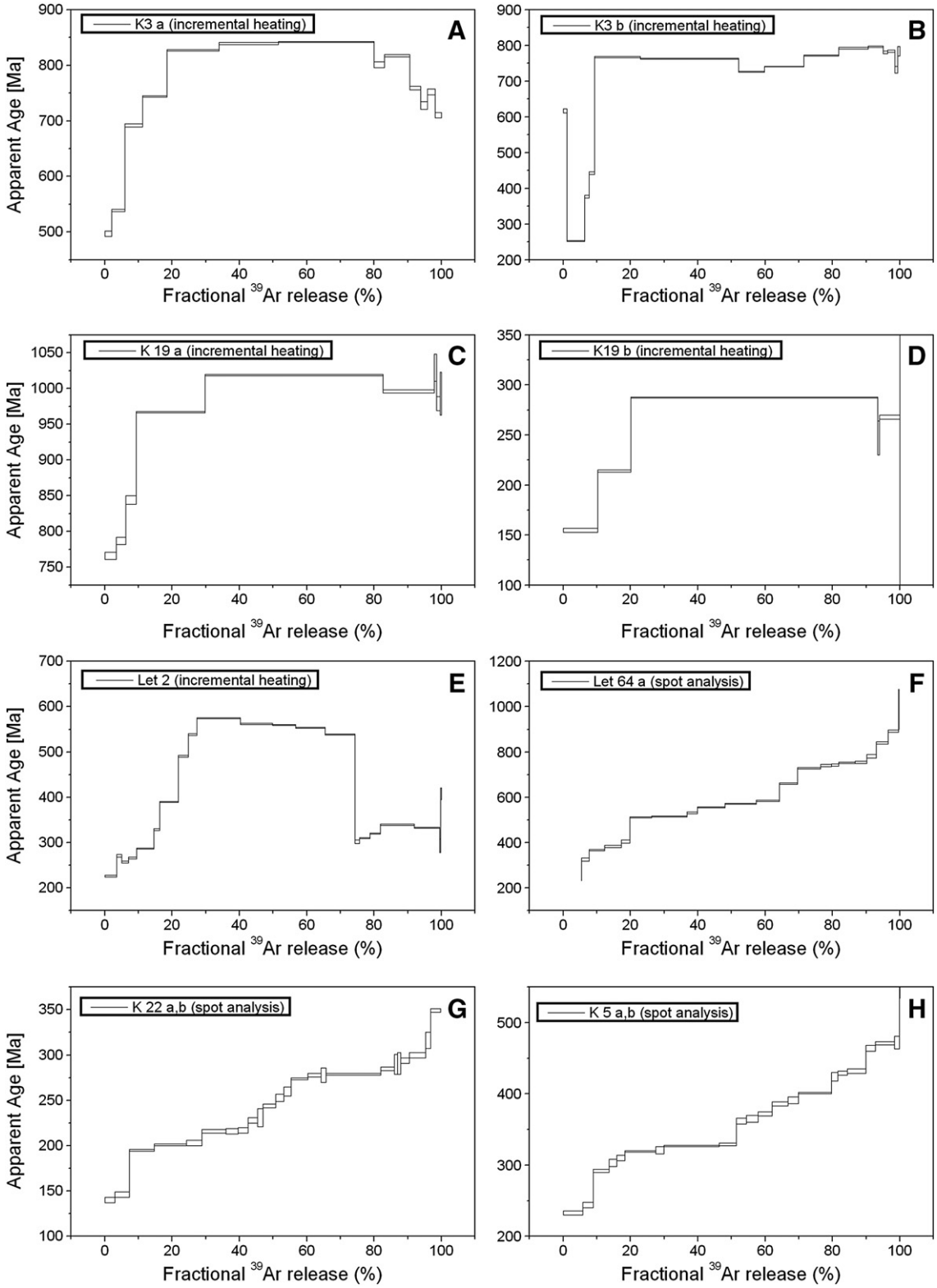

Fig. 5. A–H: Age spectra of laser spot and incremental heating analyses. The displayed laser spot ages are ordered with increasing age. The associated 'mineral age maps' can be found in the supplementary material "Lasermaps".

reached, (iv) The ages can be regarded as formation ages during one or other metasomatizing events that affected the cratonic keel through time. This requires a link to geologic / geodynamic timescales of southern Africa. In addition, we will discuss chronologic information established by other dating methods.

5.1. Comparison with other reported ^{40}Ar/^{39}Ar ages of mantle phlogopites from southern Africa

Relatively few ^{40}Ar/^{39}Ar ages from phlogopite in mantle xenoliths from southern Africa have been reported. Ages obtained with the laser

heating method on individual phlogopite grains display a similar spatial distribution as found in this study (e.g. Phillips and Onstott, 1988; Johnson and Phillips, 2003). Generally, ages tend to be older in the cores and younger at the rims of the analysed grains. The youngest ages correspond to or are close to the age of kimberlite intrusion (ca. 80–90 Ma). Reported maximum ages are: Letseng 1084±5 Ma (Wartho and Kelley, 2003), Kimberley 949±10 Ma (Johnson and Phillips, 2003); Kamfersdam c. 510 Ma (Pearson et al., 1997). The Kamfersdam kimberlite is located in the Kimberley region and of similar age, suggesting it sampled the same mantle lithosphere as the Kimberley intrusions. Wartho and Kelley (2003) also dated five phlogopites from Bultfontein with a maximum age of 803±9 Ma and four phlogopites from the DeBeers Mine with a maximum age of 1146± 20 Ma. Kaneoka and Aoki (1978) reported conventional step-heating $^{40}Ar/^{39}Ar$ data on phlogopite from xenoliths from the Kimberley group (three samples from Bultfontein Mine, two samples from Dutoitspan Mine). Their age spectra resemble those presented in this study, with ^{39}Ar recoil-induced old apparent ages obtained at lowest temperatures and elevated ages in the last, high-temperature extraction, the significance of which remains doubtful (see discussion above). However, maximum apparent ages of high-temperature extractions still agree with our results (819±14 Ma Bultfontein; 365±24 Ma Dutoitspan). Without these extractions the oldest measured age is 350±10 Ma (Bultfontein) and 183±5 Ma (Dutoitspan). The range of ages presented in this study is thus consistent with literature data.

5.2. Contributions of excess ^{40}Ar?

Reported Ar–Ar ages of phengites, biotites and phlogopites occasionally appear at odds with geologic boundary conditions, or are at least not in agreement with muscovite Ar–Ar ages and ages derived with other isotope systems for the same rock specimen (e.g. Roddick et al., 1980; Phillips and Onstott, 1986; Sherlock and Kelley, 2002). To explain this, the presence of an excess ^{40}Ar component unrelated to ^{40}K-decay in the micas was suggested. An important feature of this excess ^{40}Ar seems its homogeneous distribution in the mica lattice, mixed up with the internally produced radiogenic $^{40}Ar^*$, since the observed Ar–Ar age spectra often display nice age 'plateaus' (Roddick et al., 1980; Sherlock and Arnaud, 1999). Since this raises serious problems in interpretation of Ar–Ar age data, considerable efforts have been undertaken to explore the factors that control the incorporation of excess ^{40}Ar in mica lattice sites (e.g. Kelley, 2002; Sherlock and Kelley, 2002) and the potential use of excess ^{40}Ar in describing fluid migration kinetics at grain boundaries (Baxter, 2003).

Early studies reporting $^{40}Ar/^{39}Ar$-data of phlogopites from kimberlites or their xenoliths revealed ages older than intrusion ages (Kaneoka and Aoki, 1978; Phillips and Onstott, 1986). These 'excess' ages were attributed to the presence of excess ^{40}Ar from mantle fluids which commonly contain ^{40}Ar unsupported by K (e.g. Dunai and Baur, 1995; Hopp et al., 2007). Some xenoliths included in this study (02 Bult 2, 02 Bult 6, Kim 8, Let 39) are also part of a noble gas study (Hopp and Trieloff, 2008) and show appreciable amounts of non-atmospheric ^{40}Ar. However, these ^{40}Ar concentrations in orthopyroxene separates amount to less than 1% of the ^{40}Ar concentrations seen in our phlogopite samples, i.e. the orthopyroxenes contain no adequate amount of excess ^{40}Ar compared to phlogopite. Similarly, the laser data of a glass phase in Let 64 (supplementary material "Tables") show lower amounts of non-atmospheric ^{40}Ar ($<1.7{\cdot}10^{-18}$ mol) compared with ^{40}Ar amounts in the phlogopite ($>10^{-17}$ mol). This requires that any excess ^{40}Ar component prefers entering the phlogopite lattice compared with adjacent mineral or glass phases.

In accord with the excess ^{40}Ar hypothesis we may assume that phlogopites formed from a fluid or melt enriched in (excess) ^{40}Ar, unrelated to ^{40}K-decay, during the kimberlite event 90 Ma ago. Any earlier phlogopite formation and associated incorporation of mantle ^{40}Ar during a certain mantle residence time would require storage of this excess ^{40}Ar at mantle temperatures above its nominal closure temperature and hence, should not be retained. During intrusion and cooling of the kimberlite diffusional argon loss at low ambient argon partial pressures would occur, in agreement with the typical observed loss spectra. At the same time, the excess ^{40}Ar would increase the apparent ages and thus, obtained ages would be geologically meaningless (Kaneoka and Aoki, 1978; Phillips and Onstott, 1986, 1988). However, a common presence of excess ^{40}Ar should result in large inter-sample age variations that lack any geologic significance, but are randomly distributed. Furthermore, we expect no particular upper age limit, i.e. apparent ages exceeding any geologically constrained values (> ca. 3.5 Ga) might be possible. This expectation seems even more likely because the large observed discrepancy between the kimberlite age (90 Ma), regarded as 'true' age within this model, and our results (up to 1250 Ma) would require a dominant excess ^{40}Ar-contribution of up to 95%. Hence, a huge amount of excess ^{40}Ar would have been available to the phlogopite. There is no obvious reason why this excess ^{40}Ar concentration should reach an upper limit corresponding to an age of 1250 Ma since older apparent ages in phlogopite or biotite had been reported in literature for other locations (e.g. Kelley and Wartho, 2000). This demonstrates that any possibly existing solubility threshold must definitely correspond to a higher concentration level. Furthermore, we observe a clustering of maximum ages at 1.0–1.25 Ga, not a random age distribution. Eventually, no Ar–Ar ages >1.25 Ga have been reported in other studies for Kimberley or Lesotho so far, weakening the excess ^{40}Ar hypothesis further.

One key argument to advocate excess ^{40}Ar was that in situ radiogenic argon could not be retained at elevated mantle temperatures significantly above conventionally determined closure temperatures of argon in mica. However, Kelley and Wartho (2000) noted that possibly the concept of closure temperatures does not work for the argon system under certain circumstances. This might be the case if argon solubility in typical mantle minerals is significantly below the argon solubility in the phlogopite lattice, i.e. if the argon solid/solid partitioning coefficient is in strong favour of the phlogopite. Consequently, it had been noted that some of the reported 'excess' Ar–Ar ages formerly attributed to the presence of excess ^{40}Ar might be geologically meaningful (Pearson et al., 1997; Wartho and Kelley, 2003). We will return to this point in a later section.

5.3. Mixed ages of two or more phlogopite generations

An example of mixed ages was demonstrated for two distinct populations of white mica (phengites and muscovite) from Naxos, Greece (Wijbrans and McDougall, 1986). Ar–Ar dating of the single populations would result in a more or less well-defined age plateau but a superposition of age data caused by a composite mica aliquot will preferentially yield mixing ages without any geochronologic significance. Since phengite and muscovite differ in their argon release pattern, we expect that certain temperature extractions are dominated by one particular phase. These extractions can yield a meaningful age, namely related to the formation of the muscovite (Wijbrans and McDougall, 1986).

Mixed ages in case of our phlogopite samples might result if two or more generations of phlogopite that formed at different times before or during kimberlite emplacement are degassed within one single experiment. Our laser analysis has demonstrated that different apparent ages can be obtained from distinct phlogopite grains within a single xenolith (e.g. K 19). Those phlogopites yielding young ages are usually considered to have been thermally disturbed (during kimberlite ascent). However, if the single grain maximum ages are real, they could equally well represent younger generations of phlogopite. In contrast to the phengite-muscovite pair, the phlogopites should have similar major element compositions that result in a similar Ar-degassing pattern during stepwise heating extraction. Any mixture should then lead to a certain well-defined mixed age. The young apparent ages at lower temperatures would be due to a significant

thermally induced $^{40}Ar^*$ loss similarly affecting all phlogopite generations, whereas the progressively older apparent ages at higher temperatures would represent more closely the postulated mixed age. In order to reproduce the very restricted age range observed for our phlogopites it is necessary to mix similar proportions of phlogopite generations. Although this might be a valid scenario for several phlogopite aliquots from a single xenolith, it is highly unlikely that similar phlogopite ages would be obtained from different xenoliths by randomly mixing different phlogopite populations.

In the case of one generation of phlogopite that only shows variable late-stage Ar-loss, this loss event would be mirrored in the degassing behaviour during the experiment itself: phlogopites more prone to thermal stress will preferentially degas at lower temperatures during analysis.

5.4. Cooling ages

It is conceivable, that maximum ages represent cooling ages (i.e. the phlogopites formed much earlier in the Archean and remained at high temperatures for most of their history, preventing a closed system behaviour). In this case, all samples with similar ages should have experienced a similar thermal evolution, implying that they were stored at similar depths. A younger age (e.g. sample 02BULT 7) would suggest storage at deeper levels since closed system behaviour began later. Although this model cannot be ruled out without detailed information about the *P–T* evolution of the samples, it is unlikely that multiple samples experienced essentially the same thermal evolution path. In addition, we would expect at least some phlogopite ages older than the apparent age limit of 1.25 Ga.

5.5. Thermal resetting

Alternatively, a thermal pulse at about 1.25 Ga might have resetted the K–Ar system. This could lead to loss of the respective radiogenic $^{40}Ar^*$ accumulated in older phlogopites formed during late Archaen times during the stabilization of the cratonic lithosphere. A thermal event caused by addition of new mantle material at the base of the lithosphere or by melts intruding the lithospheric mantle was suggested by Schmitz and Bowring (2003) to account for ca. 1 Ga U–Pb ages determined in rims of zoned zircons and this had been related to zircon growth at granulite facies metamorphism during the Kibaran orogeny.

This would require that phlogopite is thermally stable enough to resist this event, but experienced total argon loss. The equilibration temperatures of our analysed specimen up to 1200 °C (Table 1) are lower than assumed maximum temperature of phlogopite stability of 1350 °C at 4–5 GPa (Trønnes, 2002). It seems unlikely that argon was lost from phlogopite at temperatures close to 1350 °C but essentially was retained up to 1200 °C for 1 Ga, in particular because the conventional closed system concept fails to explain the high 'closure temperature'. If the solid/solid partitioning behaviour of argon is the main factor in controlling its retentivity properties at given chemical and thermodynamical conditions of the mantle, one would expect no major difference throughout the whole stability range of phlogopite at all. Hence, a simple thermal heating event cannot solely account for argon loss from phlogopite within the garnet peridotite stability field but rather must be associated with either breakdown of phlogopite or the presence of pathways that enable argon transfer from lattice sites into fluidal phases (in particular melts). Such intruding or percolating melts would be representative of metasomatic impregnation. Accordingly we suggest that the dated phlogopites might represent newly formed phases during a metasomatic enrichment process 1.0–1.25 Ga ago.

5.6. Dating a major metasomatic event

This interpretation is most attractive because it can explain the rather restricted range in maximum apparent ages. All other features – variations of intergrain ages and within single grains, disturbed age spectra caused by $^{40}Ar^*$ loss – can be solely attributed to variable retentivity of the individual phlogopites at the time of incorporation of the xenoliths into the kimberlite host magma. There are two challenges with this conclusion: Has the derived age any geotectonic meaning? This point will be discussed in the next subsection. A second point is how to keep Ar stored over long time scales at ambient mantle temperatures clearly above the documented closure temperature (ca. 450 °C). This question is important for the previously discussed scenarios as well. Our preferred answer is based on the recognition of Kelley and Wartho (2000) that Ar in phlogopite might act as a closed system. There are several possibilities to achieve this. Firstly, the mineral phases in the vicinity of phlogopite might be less suitable to incorporate Ar in their lattice (i.e., Ar solubility in phlogopite is significantly higher). The solid/solid partitioning coefficient of Ar between phlogopite and orthopyroxene or olivine strongly favours the mica. Secondly, Ar-diffusivity in phlogopite under mantle *P–T* conditions could be much slower than assumed, efficiently locking the Ar within the phlogopite. In this case, the concept of closure temperatures could be still valid, if closure temperatures were several hundred degrees above current estimates.

Late-stage interaction with the kimberlite melt may lead to the breakdown of primary phlogopite. Thus, any primary phlogopite left must have resisted this late event, although probably suffering some Ar-loss. The extent of this loss is clearly dependent on local conditions (e.g. the thermal gradient within the xenolith, crack formation and melt or fluid intrusion). Argon loss might be further facilitated by a high concentration gradient between the phlogopite and melt / fluid.

The higher retentivity of argon compared with the Sm–Nd system observed for our samples (see subsection 4.3 "$^{147}Sm/^{143}Nd$-ages") might be surprising since any interaction with the kimberlite melt is expected to disturb the K–Ar system more severe than the Sm–Nd system. However, Sm–Nd ages are integrated ages derived from several grains that could be differently disturbed. It is possible, that Sm–Nd ages vary across a grain scale similar to the K–Ar system and may document a 1 Ga event in some parts of a grain. Furthermore, clinopyroxenes, garnets and phlogopite behave different concerning late-stage processes. Therefore, retentivity of both isotope systems is likely decoupled.

5.7. Geotectonic interpretation of obtained $^{40}Ar/^{39}Ar$-ages

If we accept an age constraint of about 1.0–1.25 Ga as an estimate for the time of phlogopite formation, and thus date a metasomatic event, a source of these metasomatising fluids is necessary. This could be provided by subduction related dehydration of a sinking slab during the Kibaran orogenic cycle at 1.0 to 1.25 Ga ago (Frimmel, 2004). Ascending fluids or melts enriched in water and other fluid-mobile elements like K could then lead to a progressive formation of minerals such as phlogopite that are stable at ambient *P–T* conditions of the lithospheric mantle. The present-day location of the Kimberley pipes is ~250 km from the crustal transition between ~2.5 Ga old crust and the Kibaran-aged units of the Namaquan-Natal fold belt. Subduction of a dewatering slab below the margin of the Kaapvaal craton could provide the necessary fluids even some distance from the margin. For the Lesotho xenoliths, the craton-fold-belt transition is nearby, with the host pipes having been emplaced within a small Kibaran allochthon, the Tugela terrain.

Most of our Ar–Ar ages are consistent with a major event 1 Ga ago. There is no evidence that other major geotectonic or magmatic events (e.g. the Eburnian, Pan-African, and Gondwanide orogenies or Karroo flood basalt magmatism) led to phlogopite formation within the investigated lithospheric mantle. Only sample 02 Bult 7 records an original age of about 750 Ma. This age roughly coincides with the breakup of Rodinia and could point to some magmatic disturbance of the lithospheric mantle keel at this time. However, since no other

measured phlogopites record this age, this interpretation remains speculative.

5.8. Other radiogenic isotope systems

Several radiogenic isotope systems (Rb–Sr, Sm–Nd, Lu–Hf, Re–Os, U–Pb) have been used to establish the timing of cratonic lithospheric mantle formation. All of these isotope systems are variably prone to ancient metasomatic enrichment or melt depletion events, as well as to late-stage disturbances caused by transport in the kimberlite. Therefore, individual isotope systems can provide different age information for the same rock sample. Here, we will summarize in how far ages of ca. 1.0–1.25 Ga are common for mantle xenoliths of the same lithospheric units studied in this contribution.

The Rb–Sr system appears only suited for dating the kimberlite intrusion (e.g. Allsopp and Barrett, 1975; Kramers et al., 1983; Richardson et al., 1985; Smith et al., 1994; Konzett et al., 1998). Ages obtained from garnets and clinopyroxenes from xenoliths are highly variable and frequently geologically meaningless (Simon, 2004).

The Sm–Nd system has been applied more successfully to mantle xenoliths. Richardson et al. (1984) presented Sm–Nd ages of ~3 Ga from garnet–clinopyroxene inclusion pairs in diamond and considered this as evidence for an Archean lithospheric mantle root. However, as for Rb–Sr, the Sm–Nd system in mantle xenoliths seems easily disturbed by interaction with the host kimberlite and/or metasomatic events. Accordingly, reequilibration between garnet and clinopyroxene or orthopyroxene is common (e.g. Gunther and Jagoutz, 1997; Pearson et al., 2003) and the meaning of calculated mineral isochrons remains unclear. Late-stage disturbances are documented by "future" Sm–Nd ages and ages that are younger than the kimberlite intrusion age (Simon et al., 2007). The same authors report only one grt-cpx Sm–Nd age of 202±5 Ma from the Kimberley pipe that is clearly older than the kimberlite. In the present study, all three derived Sm–Nd ages of garnet – clinopyroxene pairs are older than the kimberlite age, in the range of 115 to 355 Ma (Table 2), but the ages are still significantly younger than the respective Ar–Ar ages.

It is also possible to calculate Nd model ages assuming a chondritic uniform reservoir (CHUR) or alternatively, depleted mantle (DM) isotope evolution of the local lithosphere. This has been applied to group I and II kimberlites and their xenoliths in order to constrain the timing of metasomatic enrichment processes. Group II kimberlites tend to yield 0.6–0.9 Ga (CHUR) and 1.0–1.3 Ga (DM) model ages, the latter being in good agreement with our results (e.g. Smith, 1983; Fraser et al., 1985/86; Becker and LeRoex, 2006). However, the host kimberlites of our xenolith samples are group I, for which inferred DM and CHUR model ages are younger (less than 700 Ma). This has been interpreted as reflecting metasomatic enrichment just prior to kimberlite eruption. Our Ar–Ar age constraints are at odds with these hypothesized time differences and clearly indicate a Kibaran age of metasomatic activity.

Recently, Lu–Hf dating has revealed that this isotopic system appears much more resistant to late-stage disturbances from kimberlitic contamination than Sm–Nd. Simon et al. (2003, 2007) reported several Lu–Hf garnet–clinopyroxene two-mineral ages that fall around 1 Ga, and for three of them Ar–Ar ages are reported in this study (K3, K19, Let64). However, other samples yielded meaningless ('future') ages, and one sample recorded an age of ca. 2 Ga. It remains open, if the 1 Ga Lu–Hf ages are real and reflect the timing of a metasomatic event.

The Re–Os system is currently the radiogenic isotope system considered as most robust against contamination of xenoliths by host magma. In general, Re–Os model ages are in agreement with a late Archean formation of the Kaapvaal craton mantle (Walker et al., 1989; Pearson et al., 1995; Pearson, 1999; Irvine et al., 2001; Richardson et al., 2001; Shirey et al., 2001; Pearson et al., 2003; Carlson and Moore, 2004; Shirey et al., 2004). In detail, peridotites reveal somewhat older ages (ca. 3.0–3.3 Ga) than eclogitic parageneses (ca. 2.9 Ga) (Shirey et al., 2001, 2004). This has been regarded as a subduction related modification of the chemical composition of the cratonic lithosphere a few hundred million years after its stabilization (Richardson et al., 2001; Shirey et al., 2004). Proterozoic Re–Os model ages are less common, but present (e.g. Monastery Mine, 1.4–1.7 Ga, Carlson and Moore, 2004). So far, the limited number of Re–Os data precludes exact dating of a Proterozoic-age metasomatic event.

Finally, U–Pb dating was mainly applied to minerals from the kimberlite groundmass (e.g. perovskite, Heaman, 1989; Smith et al., 1989) or to mineral phases in the strongly metasomatised xenoliths of the 'MARID' group (mica-amphibole-rutile-ilmenite-diopside bearing xenoliths). For example, Konzett et al. (1998) dated zircons from MARID-type xenoliths and obtained U–Pb ages similar to or only slightly older than the kimberlite age, suggesting that this kind of metasomatism is a late-stage feature. Unfortunately, the U–Pb system is not suited to dating the more common and less metasomatised garnet and spinel peridotites. On the other hand, lower crustal granulite xenoliths entrained in kimberlites from both cratonic and off-craton settings can contain adequate U-bearing phases for dating (Schmitz and Bowring, 2001, 2003, 2004). In addition, application of U–Pb dating to different mineral phases with distinct closure temperatures can provide a thermochronometry of the lower crust. Not surprisingly, U–Pb zircon and monazite ages from off-craton and southwestern craton margin kimberlites (including those in northern Lesotho) point to a metamorphic imprint during the Kibaran orogeny 1.0–1.2 Ga (Schmitz and Bowring, 2001, 2004). Schmitz and Bowring (2004) also reported several zircon and rutile ages for lower crustal xenoliths contained in Mesozoic on-craton kimberlites. One of them, the Newlands kimberlite, belongs to the Kimberley group. Interestingly, the observed lower intercepts of discordant rutile ages from the lower crustal xenoliths yielded an age of ~1 Ga, whereas the zircon and monazite discordia imply late Archaen crust formation (Schmitz and Bowring, 2004). The rutile age is interpreted to reflect a tectonothermal event that reached peak metamorphic temperatures high enough to reset the rutile system (~450 °C, Schmitz and Bowring, 2003), but not the zircon system (~900 °C). This transient heating event might have been caused by melt injection into the lithospheric mantle.

6. Summary and conclusions

$^{40}Ar/^{39}Ar$ ages obtained by conventional stepwise heating technique of a series of phlogopites contained in kimberlitic mantle xenoliths from the Kimberley area (South Africa), Letseng-la-Terae and Liqhobong (both Lesotho) range from 77–1220 Ma. The shapes of high resolution age spectra can be explained by recoil redistribution of ^{39}Ar and by diffusive $^{40}Ar^*$ loss during kimberlite emplacement 90 Ma ago. The observed maximum ages cluster at 1.0–1.25 Ga. Contributions of excess ^{40}Ar, as suggested in other studies, fail to explain the coherent age range for most samples. Therefore, we consider the original ages as geologically meaningful.

$^{40}Ar/^{39}Ar$ ages obtained by laser heating are 140±3 to 1019±3 Ma, and thus within the range observed with conventional heating technique. Core ages tend to be older than ages at phlogopite rims. Both, the age distribution within single grains and the total range in ages agree with other reported laser $^{40}Ar/^{39}Ar$ data from the same locations (Pearson et al., 1997; Johnson and Phillips, 2003; Wartho and Kelley, 2003).

The majority of the xenoliths exhibits a *P–T* range of 2.9–4.6 GPa and 800–1200 °C. This is far above commonly assessed closure temperatures of phlogopite / biotite <450 °C. Following Kelley and Wartho (2000) we argue, that the solid/solid partitioning coefficient of argon in a typical mantle mineral assemblage is in strong preference for phlogopite and, at least in a dry system, argon remains metastably incorporated within the phlogopite lattice for long timescales even at high ambient temperatures in excess of its nominal closure temperature.

The age range of 1.0–1.25 Ga coincides with the Kibaran orogenic period (1.02–1.25 Ga, e.g. Frimmel, 2004) that led to the formation of the Namaqua-Natal Belt at the western and southern border of the Kaapvaal craton. This orogeny was preceded by subduction of oceanic lithosphere below the cratonic lithosphere and by formation of a juvenile island arc (Natal-Belt). We suggest that fluids or melts released during progressive subduction metasomatized the overlying mantle wedge beneath the craton and led to phlogopite formation. In particular, this scenario is capable of explaining metasomatism in the lithospheric mantle below the Kimberley area, in spite of a ca. 250 km distance to the orogenic front. Furthermore, subduction should continuously supply volatiles to the mantle wedge over an extended period of time rather than at a clear time mark. Hence, observed range in Ar–Ar ages might be not simply regarded as methodological artefact, but could indeed reflect a real spread.

We detected no age constraint that could be related to other major volcanotectonic events, e.g. breakup of Gondwana, the Karroo flood basalt magmatism, or other orogenies (Eburnian, Pan-African). A single phlogopite sample (02 BULT 7) appears to fit an age of ca. 750 Ma. If true, this could be related to the breakup of Rodinia. However, as long as no other well constrained age clusters are recognized, any further relation between geotectonic events and lithosphere evolution remains speculative.

Acknowledgements

We thank Sandra Panienka for handpicking some of the separates. Constructive comments of Ray Burgess and an anonymous reviewer improved the manuscript. JH acknowledges funding from Deutsche Forschungsgemeinschaft, grant HO 2591/1-1 and 1-3.

Appendix A. Supplementary data

Supplementary data associated with this article can be found, in the online version, at doi:10.1016/j.lithos.2008.09.001.

References

Allsopp, H.L., Barrett, D.R., 1975. Rb–Sr age determinations on South African kimberlite pipes. Physics and Chemistry of the Earth 9, 605–617.

Baxter, E.F., 2003. Quantification of the factors controlling the presence of excess ^{40}Ar and ^{4}He. Earth and Planetary Science Letters 216, 619–634.

Becker, M., LeRoex, A.P., 2006. Geochemistry of South African on- and off-craton, group I and group II kimberlites: petrogenesis and source region evolution. Journal of Petrology 47, 673–703.

Brey, G.P., Köhler, T., 1990. Geothermobarometry in four-phase lherzolites II. New thermobarometers, and practical assessment of existing thermobarometers. Journal of Petrology 31, 1353–1378.

Carlson, R.W., Moore, R.O., 2004. Age of the Eastern Kaapvaal mantle: Re–Os isotope data for peridotite xenoliths from the Monastery kimberlite. South African Journal of Geology 107, 81–90.

Carroll-Webb, S.A., Wood, B.J., 1986. Spinel–pyroxene–garnet relationships and their dependence on Cr/Al ratio. Contributions to Mineralogy and Petrology 92, 471–480.

Dunai, T., Baur, H., 1995. Helium, neon, and argon systematics of the European subcontinental mantle: implications for its geochemical evolution. Geochimica et Cosmochimica Acta 59, 2767–2783.

Foland, K.A., Xu, Y., 1990. Diffusion of ^{40}Ar and ^{39}Ar in irradiated orthoclase. Geochimica et Cosmochimica Acta 54, 3147–3158.

Fraser, K.J., Hawkesworth, C.J., Erlank, A.J., Mitchell, R.H., Scott-Smith, B.H., 1985/86. Sr, Nd, and Pb isotope and minor element geochemistry of lamproites and kimberlites. Earth and Planetary Science Letters 76, 57–70.

Frimmel, H.E., 2004. Formation of a late Mesoproterozoic supercontinent: The South Africa East Antarctica connection. In: Eriksson, P.G., Altermann, W., Nelson, D.R., Mueller, W.U., Catuneanu, O. (Eds.), The Precambrian Earth: Tempos and Events; Chapter 3, 10. Elsevier, Amsterdam.

Gaber, L.J., Foland, K.A., Corbató, C.E., 1988. On the significance of argon release from biotite and amphibole during ^{40}Ar/^{39}Ar vacuum heating. Geochimica et Cosmochimica Acta 52, 2457–2465.

Giletti, B.J., 1974. Diffusion related to geochronology. In: Hofmann, A.W., Giletti, B.J., YoderJr. Jr., H.S., Yund, R.A. (Eds.), Geochemical transport and kinetics, Publication 634. Carnegie Institution Washington, pp. 61–76.

Gunther, M., Jagoutz, E., 1997. The meaning of Sm/Nd apparent ages from kimberlite-derived coarse grained low temperature peridotites from Yakutia. Russian Journal of Geology and Geophysics 38, 229–239.

Harley, S.L., 1984. An experimental study of the partitioning of iron and magnesium between garnet and orthopyroxene. Contributions to Mineralogy and Petrology 86, 359–373.

Heaman, L.M., 1989. The nature of the subcontinental mantle from Sr–Nd–Pb isotopic studies on kimberlitic perovskite. Earth and Planetary Science Letters 92, 323–334.

Hopp, J., Trieloff, M., 2005. Refining the noble gas record of the Réunion mantle plume source: implications on mantle geochemistry. Earth and Planetary Science Letters 240, 573–588.

Hopp, J., Trieloff, M., 2008. Noble gases in kimberlitic mantle xenoliths from southern Africa. Geochimica et Cosmochimica Acta 72 (12), A389 Supplement 1.

Hopp, J., Trieloff, M., Buiklin, A.I., Korochantseva, E.V., Schwarz, W.H., Althaus, T., Altherr, R., 2007. Heterogeneous mantle argon isotope composition in the subcontinental lithospheric mantle beneath the Red Sea region. Chemical Geology 240, 36–53.

Irvine, G.J., Pearson, D.G., Carlson, R.W., 2001. Lithospheric mantle evolution of the Kaapvaal Craton: a Re–Os isotope study of peridotite xenoliths from Lesotho kimberlites. Geophysical Research Letters 28, 2505–2508.

Johnson, L., Phillips, D., 2003. ^{40}Ar/^{39}Ar dating of mantle metasomatism: A noble approach or all hot air? 8th International Kimberlite Conference Long Abstract.

Kaneoka, I., Aoki, K.-I., 1978. ^{40}Ar/^{39}Ar analyses of phlogopite nodules and phlogopite-bearing peridotites in South African kimberlites. Earth and Planetary Science Letters 40, 119–129.

Kelley, S.P., 2002. Excess argon in K–Ar and Ar–Ar geochronology. Chemical Geology 188, 1–22.

Kelley, S.P., Wartho, J.-A., 2000. Rapid kimberlite ascent and the significance of Ar–Ar ages in xenolith phlogopites. Science 289, 609–611.

Kempton, P.D., Downes, H., Neymark, L.A., Wartho, J.-A., Zartman, R.E., Sharkov, E.V., 2001. Garnet granulite xenoliths from the northern Baltic Shield—the underplated lower crust of a Palaeoproterozoic Large Igneous Province? Journal of Petrology 42, 731–763.

Konzett, J., Armstrong, R.A., Sweeney, R.J., Compston, W., 1998. The timing of MARID metasomatism in the Kaapvaal mantle: an ion probe study of zircons from MARID xenoliths. Earth and Planetary Science Letters 160, 133–145.

Kramers, J.D., Roddick, J.C.M., Dawson, J.B., 1983. Trace element and isotope studies on veined, metasomatic and "MARID" xenoliths from Bultfontein, South Africa. Earth and Planetary Science Letters 65, 90–106.

Li, J., Kornprobst, J., Vielzeuf, D., Fabriès, J., 1995. An improved experimental calibration of the olivine-spinel geothermometer. Chinese Journal of Geochemistry 14, 68–77.

Lo, C.-H., Lee, J.K.W., Onstott, T.C., 2000. Argon release mechanism of biotite in vacuo and the role of short-circuit diffusion and recoil. Chemical Geology 165, 135–166.

Marsh, J.S., Hooper, P.R., Rehacek, J., Duncan, R.A., Duncan, A.R., 1997. Stratigraphy and age of Karroo basalts of Lesotho and implications for correlations within the Karroo Igneous Province. In: Mahoney, J.J., Coffin, M.F. (Eds.), Large Igneous Provinces: Continental, Oceanic, and Planetary Flood Volcanism. Geophysical Monograph, vol. 100, pp. 247–272.

Pearson, D.G., 1999. The age of continental roots. Lithos 48, 171–194.

Pearson, D.G., Carlson, R.W., Shirey, S.B., Boyd, F.R., Nixon, P.H., 1995. Stabilisation of Archean lithospheric mantle: a Re-Os isotope study of peridotite xenoliths from the Kaapvaal craton. Earth and Planetary Science Letters 134, 341–357.

Pearson, D.G., Kelley, S.P., Pokhilenko, N.P., Boyd, F.R., 1997. Laser ^{40}Ar/^{39}Ar dating of phlogopites from southern African and Siberian kimberlites and their xenoliths: constraints on eruption ages, melt degassing and mantle volatile compositions. Russian Journal of Geology and Geophysics 38 (1), 106–117.

Pearson, D.G., Canil, D., Shirey, S.B., 2003. Mantle samples included in volcanic rocks: xenoliths and diamonds. In: Carlson, R.W. (Ed.), The mantle and core. Treatise on geochemistry. Elsevier, Amsterdam, pp. 171–275.

Phillips, D., Onstott, T.C., 1986. Application of ^{36}Ar/^{40}Ar versus ^{39}Ar/^{40}Ar correlation diagrams to the ^{40}Ar/^{39}Ar spectra of phlogopites from southern African kimberlites. Geophysical Research Letters 13, 689–692.

Phillips, D., Onstott, T.C., 1988. Argon isotopic zoning in mantle phlogopites. Geology 16, 542–546.

Reiners, P.W., Brandon, M.T., 2006. Using thermochronology to understand orogenic erosion. Annual Reviews of Earth and Planetary Science 34, 219–266.

Richardson, S.H., Guerney, J.J., Erlank, A.J., Harris, J.W., 1984. The origin of diamonds in old enriched mantle. Nature 310, 198–202.

Richardson, S.H., Erlank, A.J., Hart, S.R., 1985. Kimberlite-borne garnet peridotite xenoliths from old enriched subcontinental lithosphere. Earth and Planetary Science Letters 75, 116–128.

Richardson, S.H., Shirey, S.B., Harris, J.W., Carlson, R.W., 2001. Archaen subduction recorded by Re-Os isotopes in eclogitic sulfide inclusions in Kimberley diamonds. Earth and Planetary Science Letters 191, 257–266.

Roddick, J.C., Cliff, R.A., Rex, D.C., 1980. The evolution of excess argon in alpine biotites—a ^{40}Ar–^{39}Ar analysis. Earth and Planetary Science Letters 48, 185–208.

Schmitz, M.D., Bowring, S.A., 2001. The significance of U–Pb zircon dates in lower crustal xenoliths from the southwestern margin of the Kaapvaal craton, southern Africa. Chemical Geology 172, 59–76.

Schmitz, M.D., Bowring, S.A., 2003. Constraints on the thermal evolution of continental lithosphere from U–Pb accessory mineral thermochronometry of lower crustal xenoliths, southern Africa. Contributions to Mineralogy and Petrology 144, 592–618.

Schmitz, M.D., Bowring, S.A., 2004. Lower crustal granulite formation during Mesoproterozoic Namaqua-Natal collisional orogenesis, southern Africa. South African Journal of Geology 107, 261–284.

Schwarz, W.H., Trieloff, M., 2007. Intercalibration of ^{40}Ar–^{39}Ar age standards NL-25, HB3gr hornblende, GA1550, SB-3, HD-B1 biotite and BMus/2 muscovite. Chemical Geology 242, 218–231.

Sherlock, S.C., Arnaud, N.O., 1999. Flat plateau and impossible isochrons: Apparent ^{40}Ar–^{39}Ar geochronology in a high-pressure terrain. Geochimica et Cosmochimica Acta 63, 2835–2838.

Sherlock, S.C., Kelley, S.P., 2002. Excess argon evolution in HP-LT rocks: a UVLAMP study of phengite and K-free minerals, NW Turkey. Chemical Geology 182, 619–636.
Shirey, S.B., Carlson, R.W., Richardson, S.H., Menzies, A., Gurney, J.J., Pearson, D.G., Harris, J.W., Wiechert, U., 2001. Archean emplacement of eclogitic components into the lithospheric mantle during formation of the Kaapvaal Craton. Geophysical Research Letters 28, 2509–2512.
Shirey, S.B., Richardson, S.H., Harris, J.W., 2004. Age, paragenesis and composition of diamonds and evolution of the Precambrian mantle lithosphere of southern Africa. South African Journal of Geology 107, 91–106.
Simon, N.S.C., 2004. The formation and modification of lithospheric roots — a petrological and geochemical study of xenoliths from the Kaapvaal craton. PhD thesis, Vrije Universiteit Amsterdam, 251 pp.
Simon, N.S.C., Irvine, G.J., Davies, G.R., Pearson, D.G., Carlson, R.W., 2003. The origin of garnet and clinopyroxene in 'depleted' Kaapvaal peridotites. Lithos 71, 289–322.
Simon, N.S.C., Carlson, R.W., Pearson, D.G., Davies, G.R., 2007. The origin and evolution of the Kaapvaal cratonic lithospheric mantle. Journal of Petrology 48, 589–625.
Sletten, V.W., Onstott, T.C., 1998. The effect of the instability of muscovite during in vacuo heating on $^{40}Ar/^{39}Ar$ step-heating spectra. Geochimica et Cosmochimica Acta 62, 123–141.
Smith, C.B., 1983. Pb, Sr and Nd isotopic evidence for sources of southern African Cretaceous kimberlites. Nature 304, 51–54.
Smith, C.B., Allsopp, H.L., Garive, O.G., Kramers, J.D., Jackson, P.F.S., Clement, C.R., 1989. Note on the U–Pb perovskite method for dating kimberlites: Examples from the Wesselton and DeBeers mines, South Africa, and Somerset Island, Canada. Chemical Geology 79, 137–145.
Smith, C.B., Clark, T.C., Barton, E.S., Bristow, J.W., 1994. Emplacement ages of kimberlite occurrences in the Prieska region, southwest border of the Kaapvaal Craton, South Africa. Chemical Geology 113, 149–169.
Staudacher, Th., Jessberger, E.K., Dörflinger, D., Kiko, J., 1978. A refined ultrahigh-vacuum furnace for rare gas analysis. Journal of Physics E: Scientific Instruments 11, 781–784.
Thomas, R.J., von Veh, M.W., McCourt, S., 1993. The tectonic evolution of southern Africa: an overview. Journal of African Earth Sciences 16, 5–24.
Trieloff, M., Reimold, W.U., Kunz, J., Boer, R.H., Jessberger, E.K., 1994. $^{40}Ar–^{39}Ar$ thermochronology of pseudotachylite at the Ventersdorp Contact Reef, Witwatersrand basin. South African Journal of Geology 97, 365–384.
Trieloff, M., Weber, H.W., Kurat, G., Jessberger, E.K., Janicke, J., 1997. Noble gases, their carrier phases, and argon chronology of upper mantle rocks from Zabargad Island, Red Sea. Geochimica et Cosmochimica Acta 61, 5065–5088.
Trieloff, M., Deutsch, A., Jessberger, E.K., 1998. The age of the Kara impact structure. Russia. Meteoritic and Planetary Science 33, 361–372.
Trieloff, M., Falter, M., Jessberger, E.K., 2003. The distribution of mantle and atmospheric argon in oceanic basalt glasses. Geochimica et Cosmochimica Acta 67, 1229–1245.
Trieloff, M., Falter, M., Buikin, A.I., Korochantseva, E.V., Jessberger, E.K., Altherr, R., 2005. Argon isotope fractionation induced by stepwise heating. Geochimica et Cosmochimica Acta 69, 1253–1264.
Trønnes, R.G., 2002. Stability range and decomposition of potassic richterite and phlogopite end members at 5–15 GPa. Mineralogy and Petrology 74, 129–148.
Walker, R.J., Carlson, R.W., Shirey, S.B., Boyd, F.R., 1989. Os, Sr, Nd, and Pb isotope systematics of southern African peridotite xenoliths: Implications for the chemical evolution of subcontinental mantle. Geochimica et Cosmochimica Acta 53, 1583–1595.
Wartho, J.-A., Kelley, S.P., 2003. $^{40}Ar/^{39}Ar$ ages in mantle xenolith phlogopites: determining the ages of multiple lithospheric mantle events and diatreme ascent rates in southern Africa and Malaita, Solomon Islands. In: Vance, D., Müller, W., Villa, I. (Eds.), Geochronology: Linking the Isotope Record with Petrology and Textures. Geologic Society, vol. 220. Special Publication, London, pp. 231–248.
Wijbrans, J.R., McDougall, I., 1986. $^{40}Ar/^{39}Ar$ dating of white micas from an Alpine high-pressure metamorphic belt on Naxos (Greece): the resetting of the argon isotopic system. Contributions to Mineralogy and Petrology, 93, 187–194.
Woodland, A.B., Koch, M., 2003. Variation in oxygen fugacity with depth in the upper mantle beneath the Kaapvaal craton, southern Africa. Earth and Planetary Science Letters 214, 295–310.